Z. Phys. B 98, 207–213 (1995)

ZEITSCHRIFT
FÜR PHYSIK B

Scattering of conduction electrons by interface roughness in semiconductor heterostructures

A. Kaser, E. Gerlach

I. Physikalisches Institut, Aachen University of Technology, D-52056 Aachen, Germany

Received: 18 October 1994

Abstract. A fluctuation transport theory is applied to describe the mobility limiting effect of interface roughness scattering in semiconductor heterostructures. As an example we consider a high mobility transistor and compare electron scattering by interface roughness with Coulomb scattering processes by ions and dipole fluctuations. We show that the dynamical resistivity measurement provides detailed information about the autocorrelation of the interface morphology.

PACS: 72.20; 73.20; 73.60F

1. Introduction

The physical requirements for optoelectronic devices, e.g. the band gap for semi-conductor lasers or diodes , often cannot be fulfilled by group IV semiconductors. With the aid of novel epitaxy techniques, however, new artificial heterostructures can be grown which consist of a stack of different semiconductor materials, e.g. InGaAs/InP. The thickness of a single layer ranges from 10 Å to 1000 Å. In the region of the material with the lower intrinsic band gap a box potential is established and the quantized electron states yield a new effective band gap. Thus, the physical properties can be controlled by the thickness of the layers in the stack. However, due to thickness fluctuations of the layers the electron state lifetimes are reduced yielding limited electron mobilities in transistor devices or broadened laser lines.

In the present paper we treat the electron scattering by interface roughness in semiconductor heterostructures in a quantum mechanical context which is based on a fluctuation concept. The autocorrelation of the interface morphology plays a major role for the resulting extra resistivity. Roughness scattering compared to ion or dipole scattering turns out to be the dominant process in agreement with experiments on a HEMT[1] realized by an InGaAs/In P heterostructure. Further we show that it is possible to examine the interface morphology by a measurement of the dynamical conductivity.

[1]High electron mobility transistor

2. Theoretical concept

The different electron affinities of the atoms on both sides of a heterostructure interface lead to a dipol layer and, thus, a box potential for free carriers is established in the region of the material with the lower intrinsic band gap. We call this region conduction channel and assume that the electrons propagate freely within the channel plane ($\boldsymbol{r}$) but are confined in z-direction. Describing the intrinsic band structure of the channel material by an effective mass approximation (m) we obtain the free electron Hamiltonian

$$H_0 = -\frac{\hbar^2}{2m}\nabla^2 + V_0(z) \tag{1}$$

with a box potential $V_0(z)$ as shown in Fig. 2. In (1) we assumed the effective mass of the electron in the barrier to have the same value as in the channel. Solving the Hamiltonian by a product ansatz of planar waves and subband envelope functions $\exp(-i\boldsymbol{k}\cdot\boldsymbol{r})\cdot\varphi_n(z)$ yields the eigenvalue spectrum ($W_{k,n} = \hbar^2k^2/2m + W_n$). The binding energies of the subbands are typically of the order of several hundred meV and, thus, the extension of the wave function can reach far into the barrier and, thus, may be different from the width of the channel.

Deviations from a smooth interface, e.g. at $z = d$, are now described by a local broadening $\Delta(\boldsymbol{r})$ of the confining potential. This leads to a new potential [1]

$$V(z) = V_0\left(z\cdot\frac{d}{d+\Delta(\boldsymbol{r})}\right) \approx V_0(z) - z\frac{\Delta(\boldsymbol{r})}{d}\cdot\frac{\partial V_0(z)}{\partial z} \tag{2}$$

and a corresponding one-particle Hamiltonian with the additional scattering potential $\phi(\boldsymbol{r}, z)$:

$$H = -\frac{\hbar^2}{2m}\nabla^2 + V_0(z) + \phi(\boldsymbol{r}, z) \tag{3}$$

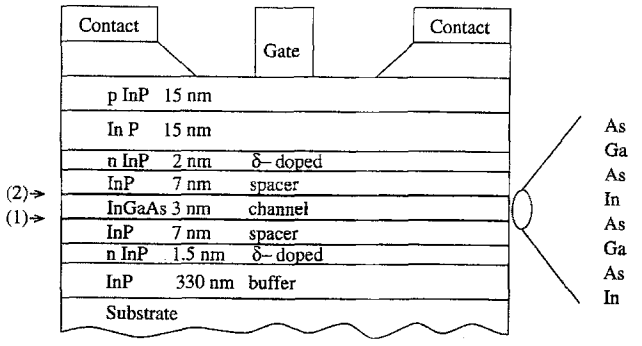

Fig. 1. The high-mobility transistor is realized as a InGaAs/InP heterostructure. The (100) growth condition guarantees a layer by layer change of the constituting atoms in the channel. The scattering by doping ions is reduced by means of the remote doping technique. The arrows indicate the channel interface positions (1) (2)

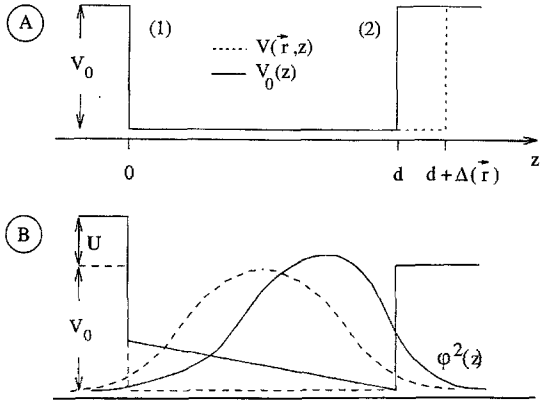

Fig. 2A, B. The interface roughness at $z = d$ is described by a local broadening $\Delta(\boldsymbol{r})$ of the confining potential $V_0(z)$ **A**. By applying a Gate-Source voltage the electron probability to stay near the interfaces is changed **B.** As a simple model we assume only the box bottom to be sloped due to a homogeneous field U/ed in the z-direction inside the channel

with

$$\phi(\boldsymbol{r}, z) = -z\frac{\Delta(\boldsymbol{r})}{d}\cdot\frac{\partial V_0(z)}{\partial z}. \tag{4}$$

We restrict ourselves to excitation frequencies lower than the subband splitting. Therefore the free electron properties can be characterized by the polarizability of the electrons of the lowest subband ($n = 1$) which is known for the non-interacting electron gas [2, 3]:

$$\Pi(\boldsymbol{k}, \omega, z, z') = \Pi_{1,1}(\boldsymbol{k}, \omega)\cdot\varphi_1^2(z)\varphi_1^2(z') \tag{5}$$

$$\Pi_{1,1}(\boldsymbol{k}, \omega) = \frac{2}{A}\sum_q \left\{\frac{f(W_{q,1})}{\hbar\omega + i\hbar 0_+ + W_{q,1} - W_{q+k,1}} - \frac{f(W_{q,1})}{\hbar\omega + i\hbar 0_+ + W_{q+k,1} - W_{q,1}}\right\}. \tag{6}$$

Now we apply the fluctuation transport concept to the present problem, and quite generally assume an oscillating external field $\boldsymbol{E}_{\text{ext}}(\omega)$ [4, 5, 6, 7, 8, 9]. The fluctuation concept uses the assumption that all electrons contribute to the macroscopic current density $\boldsymbol{j} = -en_e\boldsymbol{v}_d$ with the same drift velocity $\boldsymbol{v}_d$, where n_e is the two-dimensional electron density.This assumption allows to treat the drift of the electron resting system independently of their disordered thermal motion.

The stationary transport is characterized by a macroscopic force density balance, which takes friction, inertia and driving forces into account:

$$\boldsymbol{f}(\boldsymbol{v}_d) - mn_e\boldsymbol{v}_d - en_e\boldsymbol{E}_{\text{ext}} = 0, \tag{7}$$

$$\boldsymbol{j} = -en_e\boldsymbol{v}_d = \sigma\boldsymbol{E}_{\text{ext}}. \tag{8}$$

In the linear regime we expect the friction force to be proportional to the drift velocity and we define the friction coefficient γ by $\boldsymbol{f}(\boldsymbol{v}_d) = -\gamma\boldsymbol{v}_d$. Fourier transformation of (7) and (8) yields the frequency dependent resistivity and mobility tensor

$$\rho(\omega) = \frac{1}{n_e^2e^2}\gamma(\omega) - i\frac{m\omega}{n_ee^2}\boldsymbol{1}, \tag{9}$$

$$\mu(\omega) = -\frac{1}{en_e}\rho^{-1}(\omega). \tag{10}$$

The friction forces can be derived from a microscopic treatment of the scattering mechanism as shown in detail in [10]. Here we want to focus only on the main features of the fluctuation concept.

The fluctuations of the scattering potential in our system leads to an induced carrier density ϱ_{ind}, which gives rise to an energy dissipation of the drifting electron system. This dissipative process can be described in terms of a friction-force

$$\boldsymbol{f}(\boldsymbol{v}_d) = \frac{1}{A}\left\langle\int\varrho_{\text{ind}}(\boldsymbol{r}, z, t)\boldsymbol{E}_{\text{ind}}(\boldsymbol{r}, z, t)\mathrm{d}\boldsymbol{r}\mathrm{d}z\boldsymbol{r}\right\rangle_{\text{ens}} \tag{11}$$

where the ensemble is taken over all configurations of the statistically distributed scattering potentials e.g. of the channel width fluctuations.

The mathematical procedure is to calculate the induced charge density in its own rest system by means of a Doppler-type transformation. In this rest system screening can easily be taken into account because there the dielectric function of a non-interacting electron gas is well-known [2]

$$S(k, \omega, z, z') = \delta(z - z') - v(k)\Pi_{1,1}(k, \omega)\mathscr{L}(k, z)\varphi_1^2(z') \tag{12}$$

$$\mathscr{L}(k, z) = \int\exp(-k|z - z'|)\varphi_1^2(z')\mathrm{d}z' \tag{13}$$

$$v(k) = \frac{1}{2\varepsilon_0\varepsilon k}, \tag{14}$$

where we assumed the lattice polarizability $\varepsilon - 1$ of the channel material to have the same value as in the barrier. The screening of the scattering potential is treated within the random phase approximation and is introduced by the inverse dielectric function

$$S^{-1}(k, \omega, z, z') = \delta(z - z') + v(k)\Pi_{1,1}(\boldsymbol{k}, \omega)\cdot\frac{\mathscr{L}(k, z)\varphi_1^2(z')}{det(k, \omega)} \tag{15}$$

$$det(k, \omega) = 1 - v(k)G(k)\Pi_{1,1}(k, \omega) \tag{16}$$

$$G(k) = \int\mathscr{L}(k, z)\varphi_1^2(z)\mathrm{d}z \tag{17}$$

(12) and (17) fulfill the identity

$$\int S^{-1}(k, \omega, z, z'')S(k, \omega, z'', z')\mathrm{d}z'' = \delta(z - z'). \tag{18}$$

Under the assumption of a radially symmetric autocorrelation of the scattering potential and transport in x-direction (parallel to the plane) the procedure yields the frequency dependent scalar friction coefficient

$$\gamma(\omega) = \frac{i}{4\pi^2\omega}\int \mathrm{d}\boldsymbol{k}\, k_x^2 M(k)\frac{\Pi_{1,1}(k, \omega) - \Pi_{1,1}(k, 0)}{det(k, \omega)det(k, 0)}, \tag{19}$$

$$M(k) = \frac{1}{A}\int \langle\phi(-\boldsymbol{k}, z)\phi(\boldsymbol{k}, z')\rangle\varphi_1^2(z')\,\mathrm{d}z\,\mathrm{d}z'. \tag{20}$$

for details see [10]. We now discuss the matrix elements (20) for scattering by ions, dipole fluctuations and by interface roughness.

The remote dopant atoms are described by an ion layer density n_i at distance z_0 from the channel center. As already mentioned, the different electron affinities of the atoms on both sides of the interface lead to a dipole layer. Fluctuations of the chemical composition of the interface on an atomic scale are equivalent to statistically distributed extra dipoles which for simplicity are choosen to be oriented perpendicularly to the transport-plane and are characterized by a density n_d and a dipolmoment p.

The long range behaviour of the Coulomb potential allows one to approximate the correct subband envelope function $\varphi_1(z)$ by the simpler sine function of the infinite box potential. Thus, the matrix elements of the Coulomb scattering are given by [8]

$$\text{ions:}\quad M_i(k) = n_i\left(\frac{e^2}{2\varepsilon_0\varepsilon k}\right)^2 \exp(-2kz_0)G_i(kd/2) \tag{21}$$

$$\text{dipoles:}\quad M_d(k) = n_i\left(\frac{ep}{2\varepsilon_0\varepsilon}\right)^2 \exp(-kd_0)G_i(kd/2) \tag{22}$$

$$G_i(x) = \frac{\pi^4}{(x^2 + \pi^2)^2x^2}\sinh^2(x). \tag{23}$$

Further, inserting (4) for a box potential with barrier height V_0 in (20) yields the matrix element for roughness scattering (e.g. at the interface $z = d$):

$$\text{roughness:}\quad M_r(k) = K(k)V_0^2\varphi_1^4(d). \tag{24}$$

The matrix element M_r consists of two different factors. First there is the autocorrelation function $K(k)$ of the roughness morphology. It relates the typical length scales of the laterally extended regions of a channel width $(d + \Delta(\boldsymbol{r}))$ to the Fermi wavevector k_f (the following discussion is restricted to an exponential correlation function with a mean square roughness Δ^2 and a correlation length ξ, $K(r) = \exp(-r/\xi)$). A different ansatz would lead to a similar result. Second, in (24) there is the 'more quantum mechanical' expression $V_0\varphi_1^2(d)$ which is proportional to the probability that the electron is found at the interface. It can be expressed by the value for $V \to \infty$ times a correction factor $G_r(V)$:

$$M_r(k) = K(k)\frac{\hbar^4\pi^4}{m^2d^6}G_r(V). \tag{25}$$

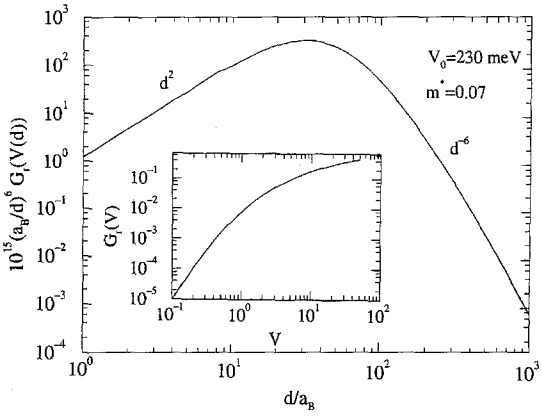

Fig. 3. Due to the correction $G_r(V)$ (insert) the thickness dependence of the roughness scattering matrix element deviates from the d^{-6} law which is obtained for an infinitely high potential barrier V_0. For a weakly bounded electron ($V \to 0$) the scattering probability is reduced as shown in the insert

$G_r(V)$ results from the transcendent energy eigenvalue equation of the Kronig–Penney model [11]:

$$G_r(V) = \frac{16}{\pi^4}\cdot\frac{x^4(V - x^2)}{(\sqrt{V - x^2} + 1)^2} \tag{26}$$

$$\text{with}\quad \tan(x) = \frac{\sqrt{V - x^2}}{x},\quad V = V_0\frac{md^2}{2\hbar^2}. \tag{27}$$

A high value of the normalized potential $V(V \gg 1)$ is equivalent to a strongly bound electron with a wavefunction that is strongly affected by channel fluctuations characterized by a correction factor of the order of one. In the opposite case of a weakly bound wavefunction $G_r(V)$ tends to zero (Fig. 3). Hence, the often discussed d^{-6} dependence of the matrix element (25) is valid only for systems with $V \gg 1$, and the influence of interface scattering on the mobility [12, 13] or on weak localization is often overestimated (Fig. 3) [14].

3. Application to dc-transport

In this section we apply our theory to a HEMT specimen (Fig. 1) [15] and compare the theoretical results with the measured mobilities (Fig. 5). The aim is the identification of the dominant scattering process in order to optimize the growth conditions in the MOVPE recctor with respect to the interface quality. The main problem concerning growth was to find the optimum reactor purging time to prevent the 'carry over' of As into the InP layer when changing the group V element from As to P [15]. Although the specimen is of high symmetry with respect to the conduction channel, the measured dc-mobility is an asymmetric function of the applied Gate–Source voltage V_{GS}.

In a first step we derive simple formulas for the dc–mobility under flat band conditions ($V_{GS} = 0$) that can serve experimentalists as a tool for a rough estimate of the

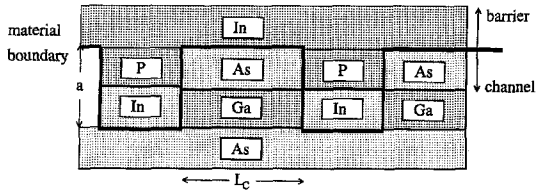

Fig. 4. Two step model for the rough interface (2). L_c is the mean lateral extension of the InGaAs channel in the interface, a the corresponding vertical extension

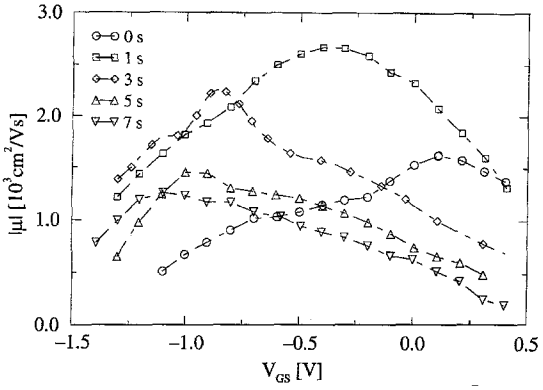

Fig. 5. The dc mobility of specimens prepared with different purging times was measured at $T = 77$ K as function of the applied Gate-Source voltage [15]. The asymmetric behaviour hints at an asymmetric scattering mechanism e.g. interface roughness scattering

mobility. The conditions for the formulas to be valid are

a) the distance z_0 between the doping layer and the center of the conduction channel must exceed the extension of the wave function (e.g. the 1/e decay of $\varphi(z)$ in the barrier),

b) $k_f d \leq 1$ should be fulfilled using approximately $G(k) \approx 1$ in the screening function (17).

Taking the limit $\omega \to 0$ in (19) the dc friction coefficient becomes

$$\gamma = -\frac{1}{4\pi^2}\int \mathrm{d}\boldsymbol{k} k_x^2 \frac{M(k)}{det^2(k,0)} \frac{\partial \Pi''_{1,1}(k,\omega)}{\partial\omega}\bigg|_{\omega=0} \tag{28}$$

$$= \frac{2k_f^2 m^2}{\pi^2\hbar^3}\int_0^{\pi/2} \mathrm{d}x \sin^4(x) \frac{M(2k_f \sin(x))}{(\sin(x)+k^*_{FT}/2k_f)^2} \tag{29}$$

with

$$\Pi_{1,1}(k,\omega) = -\frac{m}{\pi\hbar^2} - i\frac{m^2}{\pi\hbar^3 k k_f}\cdot\frac{\omega}{\sqrt{1-(k/2k_f)^2}} + \mathcal{O}(\omega^2) \tag{30}$$

and $$det(k,0) = 1 + \frac{k^*_{FT}}{k}, \quad k_{FT} = \frac{me^2}{2\pi\varepsilon_0\varepsilon}. \tag{31}$$

We obtain the following mobilities for the scattering mechanisms under consideration:

ions: $$\mu_i = \frac{qn\hbar^3(4\pi\varepsilon_0\varepsilon)^2 k_f z_0}{m^2 n_i e^4 \cdot I(2k_f z_0, k^*_{FT}/2k_f)} \tag{32}$$

Table 1. Parameters used to characterize the electron dc transport properties of the HEMT [15]

n_e [cm^{-2}]	m/m_e	ε	d [Å]	n_i [cm^{-2}]	z_0 [Å]	$n_d(p/e)^2$	Δ^2 [Å^2]	ξ [Å]
$1.5\cdot10^{12}$	0.07	12	30	$2*0.75\cdot10^{12}$	70	$4.6\cdot10^{-3}$	2.5	35

dipoles: $$\mu_d = \frac{q\hbar^3(4\pi\varepsilon_0\varepsilon)^2}{16\pi m^2 n_d e^2 p^2 \cdot D(k_f d, k^*_{FT}/1k_f)} \tag{33}$$

roughness: $$\mu_r = \frac{qnd^6}{2\pi^2\Delta^2\hbar G_r \cdot E(k_f\xi, k^*_{FT}/2k_f)} \tag{34}$$

where $$I(\alpha,\beta) = \int_0^{\pi/2} \mathrm{d}x \sin^2(x)\frac{\alpha\exp(-2\alpha\sin(x))}{(\sin(x)+\beta)^2} \tag{35}$$

$$D(\alpha,\beta) = \int_0^{\pi/2} \mathrm{d}x \frac{\sin^4(x)}{(\sin(x)+\beta)^2}\exp(-2\alpha\sin(x))\, G_i(\alpha\sin(x)) \tag{36}$$

$$E(\alpha,\beta) = \int_0^{\pi/2} \mathrm{d}x \frac{2\pi\alpha^2\sin^2(x)}{(1+4\alpha^2\sin^2(x))^{3/2}(\sin(x)+\beta)^2}. \tag{37}$$

In (34) and (37) we assumed an exponential correlation function.

Applying the specimen parameters (Table 1) to (32) we we obtain a lower limit for the mobility of $\mu_i > 150.000\ \mathrm{cm}^2/\mathrm{Vs}$ due to scattering by ions which is 6 times the measured maximum mobility $\mu_{exp} \approx 25000\ \mathrm{cm}^2/\mathrm{Vs}$. Thus, ion scattering apparently is not the dominant mechanism. Further the symmetric doping technique is in contradiction to the observed asymmetric behaviour of the mobility as a function of V_{GS}. The same argument holds also for phonon scattering.

In addition, we expect extra dipoles at the interface where the group V element changes from As to P (because of the "carry over" of As). Therefore dipole scattering may be a candidate to explain the observed asymmetric behaviour. The potential barrier V_0 at the interface can be described by a homogeneous dipole layer:

$$|V_0/e| = \frac{\eta_d \cdot p}{\varepsilon_0\varepsilon}, \quad n_d p^2 = \frac{V_0^2\varepsilon_0^2\varepsilon^2}{e^2 n_d}. \tag{38}$$

The dipole density $n_d \cdot d$ is estimated by the number of binding atomic orbitals crossing the interface in the growth direction (100). The fluctuations within the dipole layer are assumed to be uncorrelated and the upper limit for the corresponding correlation $n_d p^2$ is given by (38). With $n_d p^2 \approx 4.1 \cdot 10^{-3} e^2$ the electron mobility is at least $\mu_d > 120.000\ \mathrm{cm}^2/\mathrm{Vs}$ which is about four times the observed value. Hence, the scattering by dipoles is also negligible.

We now discuss the influence of the channel width fluctuations. If the atomic components are changed within one period of the net planes of period a, the interface morphology can be characterized by a two step model as shown in Fig. 4. If θ is the percentage of "rough" material in the interface and L_c its average lateral extension then the autocorrelation is given by

$$K(r) = a^2\theta(1-\theta)\exp(-r/\xi), \quad \xi = L_c/(1-\theta) \tag{39}$$

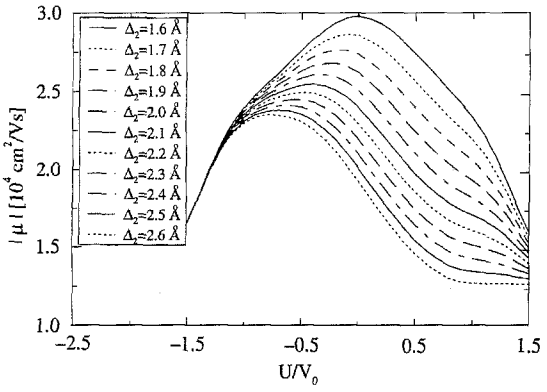

Fig. 6. The electron mobility is displayed as function of the applied potential difference U (Fig. 2b). Here we consider two rough interfaces with the same correlation length $\xi_{1,2} = 25$ Å but with different roughness depths $\Delta_1 = 1.6$ Å of interface (1) and Δ_2 as shown in the insert. Due to a positive voltage the electron wave function is pushed to the rougher interface (2) and, thus, the mobility decreases whereas it increases for opposite voltage

where we assume the probability of the lateral extensions to be a geometric distribution [16, 17]. Using the parameters $\theta = 0.5$ and $\xi = 1/k_f$ we obtain $\mu_r > 70000\,\mathrm{cm}^2/\mathrm{Vs}$. Due to the uncertainty of the channel width d of the order of 10% [18] and error up to 70 % in the calculated mobility is possible. Therefore a mobility of $30000\,\mathrm{cm}^2/\mathrm{Vs}$ is within the frame of our theory not too different from the experimental result.

Beyond the flat band approximation we calculated the dependence of the mobility on the applied Gate–Source voltage. The simple model used here is the box potential with a sloping bottom (Fig. 2) which is due to a homogeneous electric field U/ed across the channel in z-direction. The formalism discussed hitherto can be applied to this problem if the new subband wavefunctions are taken into account in the matrix elements. Figure 6 shows the theoretical predictions for the mobility under the assumption of symmetric doping and two rough surfaces with equal mean square roughness Δ^2 but different correlation length ξ. The more different the interface morphologies are the more pronounced is the asymmetric behaviour of the mobility. If the wavefunction is pushed by the sloped bottom to the rougher interface the mobility decreases and vice versa. The direction of the applied field allows the determination of the rougher interface.

Until now we have shown that electron scattering by interface roughness is a reasonable explanation of the experimentally observed properties. It is obvious that we had to make several assumptions about the morphology function. Until now, morphology data are gained by means of the photoluminescence spectroscopy [19]. In further experiments it should be tested whether these morphology data can explain the experimental transport data as outlined in our theory. Moreover we show in the next section that a measurement of the dynamical resistivity provides a powerful tool for the examination of the interface morphology.

4. Dynamical resistivity

Due to the frequency variation the dynamical resistivity measurement yields more information about the scattering process than a dc experiment. The frequency behaviour of the friction coefficient of a two dimensional electron gas is given by the polarizability and depends on the ratio $\hat{\omega} = \hbar\omega/4W_f$, W_f the Fermi-energy. Due to the plasmon dispersion curve $\omega_{pl}(k) \propto \sqrt{k}$ the plasma resonance frequency does not plays a major role for the polarizability as in three-dimensional systems. If $\hat{\omega} < 1$ the electrons follow the external electric field instantaneously and the scattering potential is screened statically, whereas for high frequencies $\hat{\omega} > 1$ the screening breaks down. In the intermediate region collective plasma excitations give rise to an extra resistivity that has already been observed in semiconductor bulk specimens with the aid of infrared spectroscopy [20, 21, 23]. The spectroscopic measurement of the macroscopic susceptibility of the free carriers

$$\chi_{FC}(\omega) = \frac{i}{\rho(\omega)\varepsilon_0\omega} = \frac{q^2 n_e^2}{d\varepsilon_0\omega}\cdot\frac{\gamma''(\omega) - \mathrm{i}m n_e\omega + \mathrm{i}\gamma'(\omega)}{\gamma^2(\omega) + (\gamma''(\omega) - m n_e\omega)^2} \tag{40}$$

$$\to \underbrace{\frac{e^2 n_e}{\varepsilon_0 m d\omega^2}}_{\text{inertia}} + \underbrace{\frac{e^2\gamma'(\omega)}{\varepsilon_0 m^2 d\omega^3}}_{\text{friction}} \quad \text{for} \quad m n_e\omega \gg |\gamma(\omega)| \tag{41}$$

provides the high frequency limit ($m n_e\omega > |\gamma(\omega)|$) of the real part of the friction coefficient, that has different frequency dependences for various scattering mechanisms [21, 22]. In the limit under consideration (19) yields for the real part

$$\gamma'\omega = -\frac{1}{4\pi^2\omega}\int \mathrm{d}\boldsymbol{k} k_x^2 M(\boldsymbol{k})\Pi''_{1,1}(k,\omega), \quad \hbar\omega \gg 4W_f \tag{42}$$

$$\Pi''_{1,1}(k,\omega) = -\frac{m}{2\pi\hbar^2\hat{k}}\sqrt{1-(\hat{k}-\hat{\omega}/\hat{k})^2}, \quad \text{with } |\hat{k}-\hat{\omega}/\hat{k}| < 1 \tag{43}$$

$$\hat{k} = k/2k_f,\ \hat{\omega} = \hbar\omega/4W_f$$

$$\Rightarrow \gamma'(\omega) = \frac{m^2 k_f^2}{8\pi\hbar^3} M(k), \quad k = \sqrt{\hat{\omega}}\cdot 2k_f, \tag{44}$$

which directly allows the determination of the matrix element wavevector dependence.

The following discussion is based on the resistivity because it is more intuitive than a friction coefficient, see (9). In the system under consideration we find the following behaviour of the resistivity for scattering by ions, dipoles and roughness, respectively:

$$\rho'_i(\omega) = \rho_i^\dagger\cdot\frac{1}{x^2}\frac{\pi^4\exp(-4xz_0/d)}{(x^2+\pi^2)^2x^2}\sinh^2(x)$$

$$\to \propto \exp(-2\sqrt{\hat{\omega}}k_f(2z_0 - d)) \tag{45}$$

$$\rho'_d(\omega) = \rho_i^\dagger\cdot\frac{\pi^4}{(x^2+\pi^2)^2x^2}(1-\exp(-2x))^2 \to \propto \hat{\omega}^{-3} \tag{46}$$

$$\rho'_r(\omega) = \rho_r^\dagger 2\pi\cdot(1+4\hat{\omega}(k_f\xi)^2)^{-3/2} \to \propto \hat{\omega}^{-3/2} \tag{47}$$

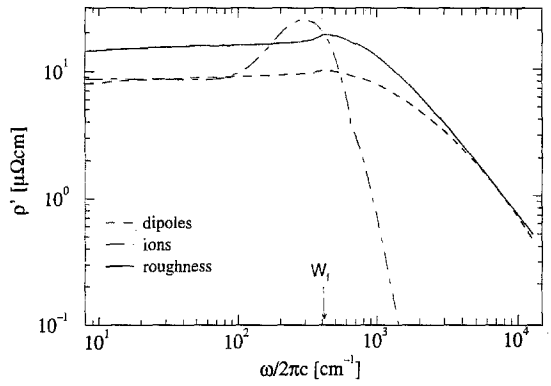

Fig. 7. Theoretical predictions for the contributions of the discussed scattering mechanisms to the real part of the resistivity. The extra resistivity near W_f is due to collective plasma excitations

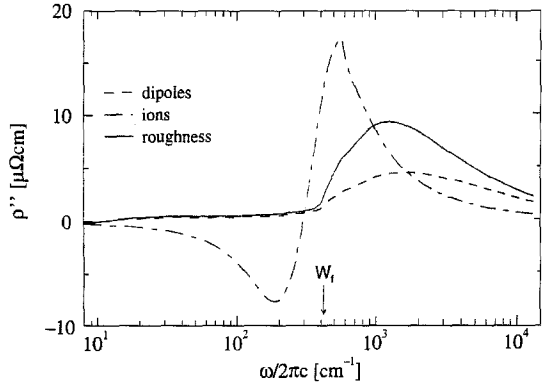

Fig. 8. Theoretical predictions for the imaginary part of the resistivity (compare with Fig. 7)

with

$$\rho_i^{\dagger} = \frac{m^2 n_{io} e^2 d^3}{64\varepsilon_0^2 \varepsilon^2 \hbar^3 n_e}, \rho_r^{\dagger} = \frac{\pi^2 \hbar \Delta^2 \xi^2}{4 n_e q^2 d^5} G_r(V), x = \sqrt{\hat{\omega}} k_f d. \quad (48)$$

While the scattering by doping ions decreases exponentially with increasing frequency the dipole and interface roughness scattering can be distinguished due to their different power laws. The correlation length ξ and the mean square roughness Δ^2 can be estimated by means of a log-log plot.

Beyond this high frequency approximation we calculated numerically the resistivity and the corresponding macroscopic susceptibility over a wide frequency range as shown in Figs. 7 to 10. The extra resistivity near $\hat{\omega} \approx 0.25$ is due to the excitations of collective plasma oscillations.

Experimental results are often described by a Drude approximation of the free carrier susceptibility $\chi_{FC,Drude}$ with a frequency independent scattering time ω_τ^{-1}.

$$\chi_{FC,Drude} = -\frac{n_e e^2}{d\varepsilon_0 m\omega} \cdot \frac{1}{\omega + i\omega_\tau} \quad (49)$$

Comparison of our results with (49) leads to an interpretation of a frequency dependent scattering time.

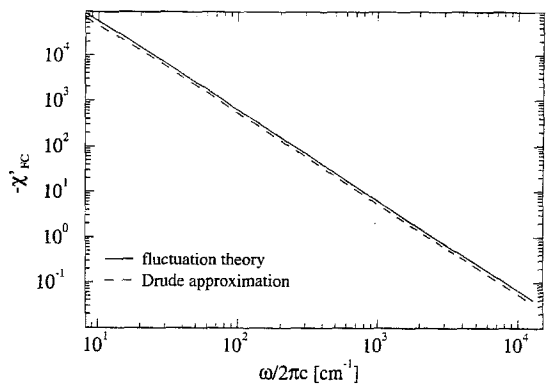

Fig. 9. Theoretical predictions for the real part of the macroscopic electron susceptibility. The Drude behaviour is characterized by the scattering frequency which can be derived from the dc-properties of the resistivity. χ'_{FC} is dominated by the inertia of the electrons and, thus, there is no difference between Drude approximation and our theory

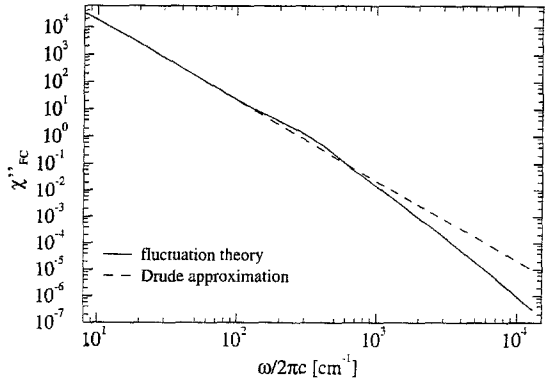

Fig. 10. Theoretical predictions for the imaginary part of the electron macroscopic susceptibility. The deviation from Drude like behaviour is due to a frequency dependent scattering frequency which is calculated by the fluctuation theory. The different frequency power laws allow the identification of the dominant scattering process

5. Summary

We have shown how the mobility of a two-dimensional election gas is affected by interface roughness and have compared this mechanism with the Coulomb scattering processes. Our formalism was applied to a high mobility transistor, and here the interface roughness was found to be the mobility limiting scattering mechanism in dc-transport. In a second step we calculated the dynamical transport properties and found the dynamical resistivity measurement to be a powerful tool for the determination of the strongest scattering mechanism. If roughness scattering is dominant this technique in addition to photoluminescence spectroscopy yields a powerful tool to measure the interface morphology parameter Δ^2 independently of the correlation length ξ. It is an open question whether the morphology data obtained by these two different techniques are consistent with each other.

The authors are very indebted to Prof. P. Grosse and Dipl. Phys. A. Kohl for their interest in our work and their stimulating discussions.

References

1. Tešanović, Z. et al.: Phys. Rev. Lett. **57**, 2760 (1986)
2. Backes, W. et al.: Phys. Rev. B **45**, 8437 (1991)
3. Ando, T., Fowler, A.B., Stern, F.: Rev. Mod. Phys. **54**, 450 (1982)
4. Gerlach, E., Mycielski, J.: Verh. Dtsch. Phys. Ges. **17**, 746 (1982)
5. Gerlach, E., Mycielski, J.: private communication
6. Gerlach, E.: Phys. Statics. Solid. (b) **158**, 531 (1990)
7. Gerlach, E.: Phys. Statics. Solid. (b) **157**, 189 (1990)
8. Gerlach, E.: Phys. Statics. Solid. (b) **167**, 233 (1991)
9. Hertling, R.: Diploma thesis RWTH-Aachen 1993
10. Kaser, A., Gerlach, E.: Z. Phys. B **97**, 139 (1995)
11. Merzbacher, E.: Quantum mechanics New York: Wiley 1970
12. Sakaki, H., et al.: Appl. Phys. Lett. **51** 1934 (1987)
13. Bolognesi, C.R., Kroemer, H., English, J.H.: Appl. Phys. Lett. **61**, 213 (1992)
14. Gold, A.: Solid State Commun. **60**, 531 (1986)
15. Kohl, A., et al.: Vth International Conference on InP and related Materials, Paris (1993), IEEE Nr: 93Ch3276-3
16. Busch, H., Henzler, M.: Surf. Sci. **167**, 534 (1986)
17. Pukite, P.R., Lent, C.S., Cohen, P.I.: Surf. Sci. **161**, 39 (1986)
18. Kohl, A.: Private communication
19. Herman, M.A., Bimberg, D., Christen, J.: J. Appl. Phys. **70**, R1 (1991)
20. Gerlach, E. et al.: Phys. Statics Solid: (b) **75**, 553 (1976)
21. Gerlach, E., Grosse, P.: Festkörperprobleme XVII. Berlin, Heidelberg, New York: Springer 1977
22. Gerlach, E.: J. Phys. C **19**, 4585 (1986)
23. Kluttig, H.: Thesis RWTH-Aachen, Germany 1982